Chapter 15

INTERSPECIFIC AND INTRASPECIFIC TAXONOMIC AFFINITY BASED ON PERMANENT MANDIBULAR MOLAR ENAMEL-DENTINE JUNCTION MORPHOLOGY OF THE SCLADINA I-4A JUVENILE

Dorien DE VRIES, Jean-Jacques HUBLIN, Michel TOUSSAINT & Matthew M. SKINNER

Michel Toussaint & Dominique Bonjean (eds.), 2014. The Scladina I-4A Juvenile Neandertal (Andenne, Belgium), Palaeoanthropology and Context
Études et Recherches Archéologiques de l'Université de Liège, 134: 315-324.

1. Introduction

Dental crown morphology is often used to assess the taxonomic affinity and phylogenetic relationship of individual specimens. In a number of studies molar crown morphology has been found to discriminate between extant hominoid species and sub-species (Johanson, 1974; Uchida, 1992, 1996; Pilbrow, 2003, 2006) and extinct hominoid taxa (Weidenreich, 1937; Robinson, 1956; Sperber, 1974; Wood & Abbott, 1983; Suwa, 1996; Bailey, 2002, 2006; Irish & Gautelli-Steinberg, 2003; Grine, 2004; Hlusko, 2004; Guatelli-Steinberg & Irish, 2005). However, the effects of dental attrition on the outer enamel surface can decrease the taxonomic information of external crown morphology and necessitate the use of less comprehensive measures of tooth crown shape (e.g. linear crown measurements).

Recently, it has been demonstrated that the internal structure of the tooth crown, and in particular the enamel-dentine junction (EDJ), retains considerable taxonomic information in variably worn fossil teeth (e.g. Corrucini, 1987, 1998; Olejniczak et al., 2004, 2007; Macchiarelli et al., 2006; Suwa et al., 2007; Skinner et al., 2008) and is able to discriminate chimpanzee species and subspecies (Skinner et al., 2009). In particular, this is because the EDJ retains valuable information on vertical crown components, such as relative/absolute dentine horn height and crown height, which have been lost in the external crown morphology of worn teeth. The EDJ can therefore be used to assess the taxonomic and phylogenetic position of individual specimens, populations, and species.

In this contribution we address three questions: 1) is the EDJ morphology of the mandibular molars consistent with the classification of Scladina I-4A as a Neandertal, 2) are there consistent differences in EDJ morphology between Early and Classic Neandertals, and 3) is the morphology of the EDJ of the Scladina specimen consistent with other Neandertals of a similar geochronological age. We use micro-computed tomography to image the EDJ; geometric morphometric analysis to capture the shape of the EDJ; and multivariate analyses to compare the EDJ morphologies among the different taxa.

2. Materials and methods

The materials used for this study are outlined in Table 1. The comparative sample consists of a large number of Neandertal specimens (n = 47), fossil *Homo sapiens* (n = 19), and recent *Homo sapiens* (n = 55). Specimens that exhibited an abnormal morphology were excluded from the comparative sample. In the case of antimeres being present for a specimen the side that was better preserved was used in the analysis. The references cited in Table 1 were used to establish the taxonomy and tooth position of each specimen. Additionally, the tooth position of all specimens, based on EDJ shape, was evaluated. Specimens whose classification was inconsistent were excluded from the comparative sample. If specimens were consistently classified to a molar position that was different than previously published, the specimen was reclassified based on the EDJ results (and listed with a '4' in the 'Tooth' column in Table 1).

Geometric morphometric analysis

The molars of our comparative sample were subjected to micro-CT scanning using both industrial and desktop micro-CT systems with resultant voxel resolutions ranging from 14 to 70 µm. The image stack of each scan was filtered using a three-dimensional median and mean-of-least variance filter to facilitate segmentation (using Avizo 6.3) into enamel and dentine components. The enamel-dentine junction was exported as a .ply surface model for the collection of landmarks

Specimen (*n* = 121)	Tooth	Side	Basis	Molar ref	Source
***Homo neanderthalensis* (*n* = 47)**					
Abri Suard 5	1	L	1	—	TNT
Abri Suard 14_7	1	R	2	1	TNT
Abri Suard 43	3	R	3	1	TNT
Abri Suard 36	2	L	1	—	TNT
	3	L	1	–	TNT
Abri Suard 49	1	R	3	1	TNT
Combe-Grenal I	1	R	1	–	MNP
Combe-Grenal IV	1	L	1	–	MNP
Combe-Grenal XII	3	L	3	2	MNP
El Sidron SD540	2	L	2	3	MNCN
El Sidron SD755	2	R	4	–	MNCN
El Sidron SD780	1	L	2	3	MNCN
El Sidron SD1135	3	R	1	–	MNCN
Krapina 52	1	L	1	–	CMNH
Krapina 53	1	R	1	–	CMNH
	2	R	1	–	CMNH
	3	R	1	–	CMNH
Krapina 54	1	L	1	–	CMNH
	2	L	1	–	CMNH
Krapina 55	1	L	1	–	CMNH
	2	L	1	–	CMNH
Krapina 57	2	R	1	–	CMNH
	3	R	1	–	CMNH
Krapina 59	2	R	1	–	CMNH
Krapina D1	2	R	2	4	CMNH
Krapina D6	2	L	2	4	CMNH
Krapina D9	2	L	3	4	CMNH
Krapina D79	1	R	2	4	CMNH
Krapina D80	2	R	3	4	CMNH
Krapina D81	1	L	2	4	CMNH
Krapina D86	2	L	3	4	CMNH
Krapina D104	3	R	3	4	CMNH
Krapina D105	2	L	3	4	CMNH
Krapina D106	3	L	2	4	CMNH
Krapina D107	2	L	2	4	CMNH
Lakonis	3	L	3	5	EPSNE
La Quina H9	2	L	1	–	TNT
	3	L	1	–	TNT
Le Moustier	1	L	1	–	NMP
	2	L	1	–	NMP
	3	L	1	–	NMP
Le Regourdou	2	L	1	–	MAA
	3	L	1	–	MAA
Roc de Marsal	1	R	1	–	MNP
Saint-Césaire 1	3	R	1	–	MAN
Vindija 11_39	2	R	1	–	CNHM
	3	R	1	–	CNHM
Pleistocene *Homo sapiens* (*n* = 19)					
Dar es Soltane 2 H4	2	L	1	–	INSAP
	3	L	1	–	INSAP
El Harhoura	2	R	1	–	INSAP
	3	R	1	–	INSAP
Equus Cave H3	3	R	4	–	MM
Irhoud 3	1	L	1	–	UM
	2	L	1	–	UM
	3	L	1	–	UM
Oberkassel D999.02	2	L	1	–	LVRB
	3	L	1	–	LVRB
Qafzeh 9	1	L	1	–	SSM
	2	L	1	–	SSM
	3	L	1	–	SSM
Qafzeh 10	2	L	1	–	TAU
Qafzeh 11	2	L	1	–	TAU
Qafzeh 15	1	L	1	–	TAU
	2	L	1	–	TAU
Temara mandible	2	L	1	–	INSAP
	3	L	1	–	INSAP
Recent *Homo sapiens* (*n* = 55)					
Belgian A31	1	R	1	–	RBINS
Belgian A32	1	R	1	–	RBINS
Belgian 13e	2	R	1	–	RBINS
Belgian 76a	2	L	1	–	RBINS
Belgian 89a	1	L	1	–	RBINS
Belgian 93a	1	L	1	–	RBINS
Belgian 129a	1	L	1	–	RBINS
MPI M3	1	L	1	–	MPI–EA
MPI M5	1	L	1	–	MPI–EA
MPI M71	3	L	1	–	MPI–EA
MPI M131	3	R	1	–	MPI–EA
MPI M132	3	L	1	–	MPI–EA
MPI M133	3	L	1	–	MPI–EA
MPI M135	3	L	1	–	MPI–EA
MPI M146	2	L	1	–	MPI–EA
MPI M162	2	R	1	–	MPI–EA
MPI M190	2	L	1	–	MPI–EA
MPI M213	3	L	1	–	MPI–EA
Romanian R123	1	L	1	–	IA
Romanian R167_I75	1	L	1	–	IA
Romanian R258_144	1	L	1	–	IA
Romanian R488_274	1	L	1	–	IA
Romanian R605_1185	1	L	1	–	IA
	3	R	1	–	IA
Romanian R1101_1498	1	R	1	–	IA
	3	L	1	–	IA
Romanian R1160_440	1	L	1	–	IA
Romanian R1586_2425	3	L	1	–	IA
Romanian R1620_2480	3	R	1	–	IA
Romanian R1719_1237	3	L	1	–	IA
Romanian R1989_1382	1	L	1	–	IA
	2	L	1	–	IA
Romanian R2070_1423	2	R	1	–	IA
Romanian R2525_1641	2	L	1	–	IA
Romanian R2602_1673	1	L	1	–	IA
NMNH SI12	1	R	4	–	NMNH
NMNH SI13	1	L	4	–	NMNH
NMNH SI15	1	R	4	–	NMNH
NMNH SI34	1	L	4	–	NMNH
NMNH SI36	1	L	4	–	NMNH
NMNH SI37	1	L	4	–	NMNH
NMNH SI38	1	L	4	–	NMNH
NMNH SI40	1	L	4	–	NMNH
NMNH SI42	1	R	4	–	NMNH
NMNH SI44	1	R	4	–	NMNH
NMNH SI45	1	R	4	–	NMNH
NMNH SI46	1	R	4	–	NMNH
NMNH SI47	1	R	4	–	NMNH
NMNH SI48	1	R	4	–	NMNH
ULAC 58	1	L	1	–	ULAC
	3	L	1	–	ULAC
ULAC 179	3	R	1	–	ULAC
ULAC 536	3	L	1	–	ULAC
ULAC 790	3	L	1	–	ULAC
ULAC 797	1	R	1	–	ULAC

Table 1 (facing page): Comparative sample, showing for each specimen the tooth position and side, basis of tooth position certainty, tooth position reference, and source of specimen.

Basis: 1 – specimen is in jaw; 2 – associated dentition; 3 – estimate based on morphology; 4 – classified through geometric morphometric analysis in this study. **Molar references**: 1. Teilhol, 2001; 2. Garralda & Vandermeersch, 2000; 3. Rosas, 2009; 4. Radovčić et al., 1988; 5. Harvati et al., 2003. **Source**: CMNH – Croatian Museum of Natural History; EPSNE – Ephorate of Palaeoanthropology & Speleology of Southern Greece; GPIH - Geologisch-Paläontologisches Institut der Universität Heidelberg; IA – Francisc J. Rainer Institute of Anthropology; INSAP – Institut National des Sciences de l'Archéologie et du Patrimoine; LVRB – Landschaftsverband Rheinland – LandesMuseum Bonn; MA – Le Musée d'Agoulème, France; MAA – Musée d'Art et d'Archéologie du Périgord; MAN – Musée d'Archéologie nationale de Saint-Germain-en-Laye; MM – McGregor Museum, Kimberley; MNCN – Museo Nacional de Ciencias Naturales; MNP – Musée National de Préhistoire, France; MPI-EVA – Max Planck Institute for Evolutionary Anthropology; MVFB – Museum für Vor- und Frühgeschichte Berlin; NMNH – National Museum of Natural History; RBINS – Royal Belgian Institute of Natural Sciences; SMF – Senckenberg Forschungsinstitute und Naturmuseum; SSM – Sackler School of Medicine; TAU – Tel Aviv University; TNT – The Neanderthal Tools project of the Neanderthal Studies Professional Online Service (NESPOS); ULAC – Universität Leipzig, Institut für Anatomie, Lehrsammlung Anatomie; UM – University Mohammed V-Agdal, Rabat.

in Avizo 6.3. Worn teeth of which small portions of the dentine horns were incomplete were reconstructed in Geomagic Studio 10. Molars that showed evidence of significant damage, missing areas, or an abnormal (i.e. pathological) morphology were excluded from this study.

Three sets of landmarks were collected on each EDJ surface (Figure 1): 1) the CEJ RIDGE, capturing the shape of the cementum-enamel junction of the tooth crown starting at the mesiobuccal corner moving lingually; 2) the EDJ MAIN, placed on the dentine horn tips of the protoconid, metaconid, entoconid, and hypoconid, respectively; and 3) the EDJ RIDGE, capturing the EDJ ridge that connects the dentine horns starting at the protoconid and moving lingually.

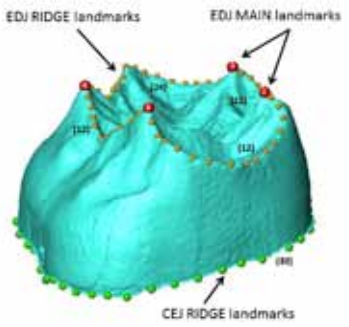

Figure 1: The three landmark sets illustrated on the EDJ surface of the Scladina permanent mandibular right second molar Scla 4A-1/M_2. The EDJ MAIN landmarks are pictured as red dots, located on the top of the four main dentine horns (numbers showing the order of collection). The EDJ RIDGE landmarks start at the protoconid (MAIN landmark number 1), the CEJ RIDGE starts at the mesiobuccal corner. The EDJ and CEJ ridges consist of an arbitrary number of landmarks, which are later replaced by a fixed number of equally spaced semi-landmarks in Mathematica. The number in brackets refers to the number of semi-landmarks after the derivation of homologous landmarks in Mathematica, the landmarks shown here are the original landmarks.

For each specimen a single set of homologous landmarks was created in Mathematica v8.0 following methods outlined in Skinner (2008) and Skinner & Gunz (2010). Briefly, a smooth curve was interpolated for both the CEJ and EDJ RIDGE landmark sets using a cubic-spline function. On each curve a fixed number of equidistantly-spaced landmarks was placed (30 for the CEJ RIDGE and 60 for the EDJ RIDGE, see Figure 1). The EDJ MAIN landmarks were treated as landmarks, whereas the former ridge landmarks were treated as semi-landmarks. Semi-landmarks were subjected to sliding (described in Gunz et al., 2005) and, finally, the landmark set of each specimen were converted to shape coordinates by generalized least squares Procrustes superimposition (Gower, 1975; Rohlf & Slice, 1990).

A principal component analysis (PCA) of the shape coordinates was used to assess the shape variation of the different groups at each molar position (see Figure 2). A canonical variate analysis (CVA) was used to find the axes that best separate groups, illustrating the minor but consistent differences in EDJ morphology between groups. As classification based on a CVA can differ for the same specimen depending on the number of PCs used, we report the cross-validated classification results of each specimen using each of 5-20 PCs. PCA, CVA, and classification were all carried out in R and groups were assigned equal prior probabilities.

Intraspecific temporal variation in EDJ morphology of the Neandertal sample was assessed by splitting the sample into Early Neandertals and Classic Neandertals; early being all specimens dated to >100,000 years and classic being all specimens dated to <100,000 years. This date was

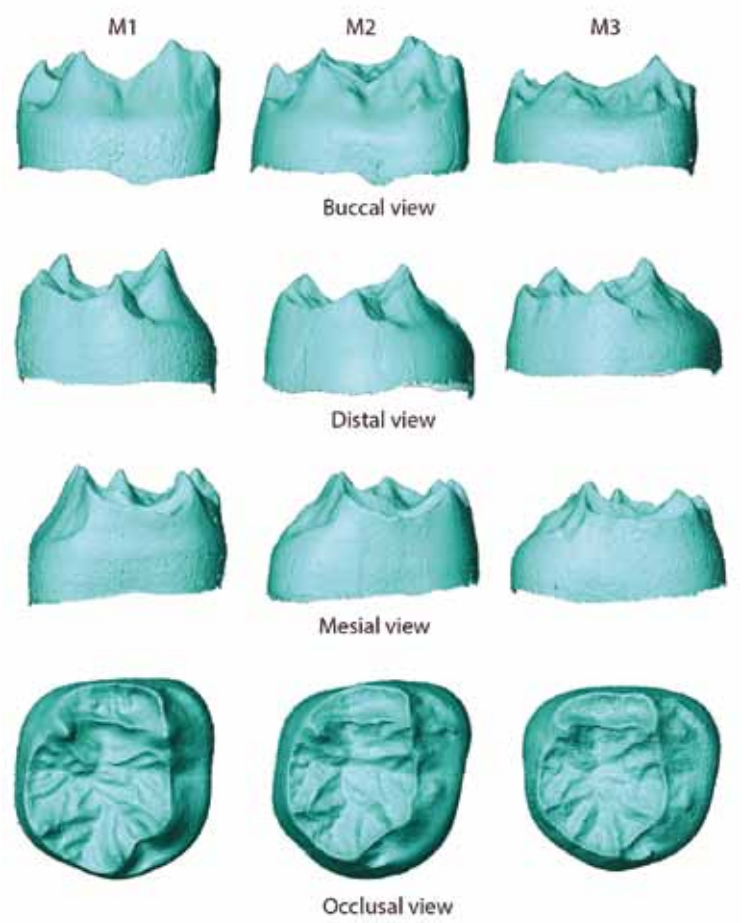

Figure 2: Scladina EDJ morphology of permanent mandibular right molars (Scla 4A-1/M_1, M_2 & M_3) in buccal, distal, mesial, and occlusal view.

chosen based on previous studies assessing the morphological transitions inherent to an accretion of Classic Neandertal morphology (e.g. Dean et al., 1998; Hublin, 1998, 2009; Harvati et al., 2010**).**

We used a Mann-Whitney U Test to determine if tooth size (measured as the natural log of centroid size) differed significantly between groups. The Neandertal and Pleistocene Modern Human groups did not differ significantly in log centroid size (p = 0.161 for the M_1, p = 0.754 for M_2, and p = 0.934 for M_3). When the Neandertal group was split into Early and Classic Neandertal groups, the log centroid size of these groups also did not differ significantly (p = 0.721 for M_1, p = 0.639 for M_2, and p = 0.598). Therefore, we restrict the results presented here to those in *shape* space only, excluding log centroid size as part of the CVA. However, we examined the results in *form* space (see Gunz et al., 2012) and the results were broadly similar.

3. Results

3.1. Classification of Scladina among Late Pleistocene *Homo* (Table 2)

Based on the geometric morphometric analysis of the EDJ of the permanent mandibular molars, the Scladina specimen (Figure 3) classifies consistently as a Neandertal. The M_1 and M_2 are classified as Neandertal 100% of the time. The M_3 classifies as a Neandertal 56% of the time and as a Recent Modern Human 44% of the time (in *form* space 69% and 31%, respectively).

3.2. Temporal variation in Neandertal molar EDJ morphology (Table 3)

The Neandertal sample was divided into Early and Classic Neandertals, based on their geochronological age. The majority of the Neandertal specimens were classified correctly into Early and Classic Neandertals according to their geochronological age (Table 3). These results indicate that there are subtle but consistent differences in Early and Classic Neandertal permanent mandibular molar EDJ morphology. A small number of specimens did not classify as expected and classified inconsistently with their geochronological

Hs = recent *Homo sapiens*, **Hsp** = Pleistocene *Homo sapiens*, **Hn** = *Homo neanderthalensis*, **Hne** = Early Neandertal, **Hnc** = Classic Neandertal.

M_1	Accuracy	M_2	Accuracy	M_3	Accuracy
Hs (32)	97%	Hs (8)	88%	Hs (15)	93%
Hsp (3)	100%	Hsp (9)	100%	Hsp (7)	100%
Hn (14)	100%	Hn (18)	100%	Hn (14)	100%

Table 2: Classification accuracy of Late Pleistocene *Homo* shown as the percentage of correctly classified specimens for each group. A specimen was considered classified correctly when at least 75% of analyses (using each of 5-20 PCs) classified the specimen correctly.

M_1	Accuracy	M_2	Accuracy	M_3	Accuracy
Hs (32)	97%	Hs (8)	100%	Hs (15)	93%
Hsp (3)	100%	Hsp (9)	100%	Hsp (7)	100%
Hne (9)	89%	Hne (13)	92%	Hne (6)	67%
Hnc (5)	100%	Hnc (6)	100%	Hnc (8)	100%

Table 3: Classification accuracy when Early and Classic Neandertals are treated as two separate groups, shown as the percentage of correctly classified specimens for each group. A specimen was considered classified correctly when at least 75% of analyses (using each of 5-20 PCs) classified the specimen correctly.

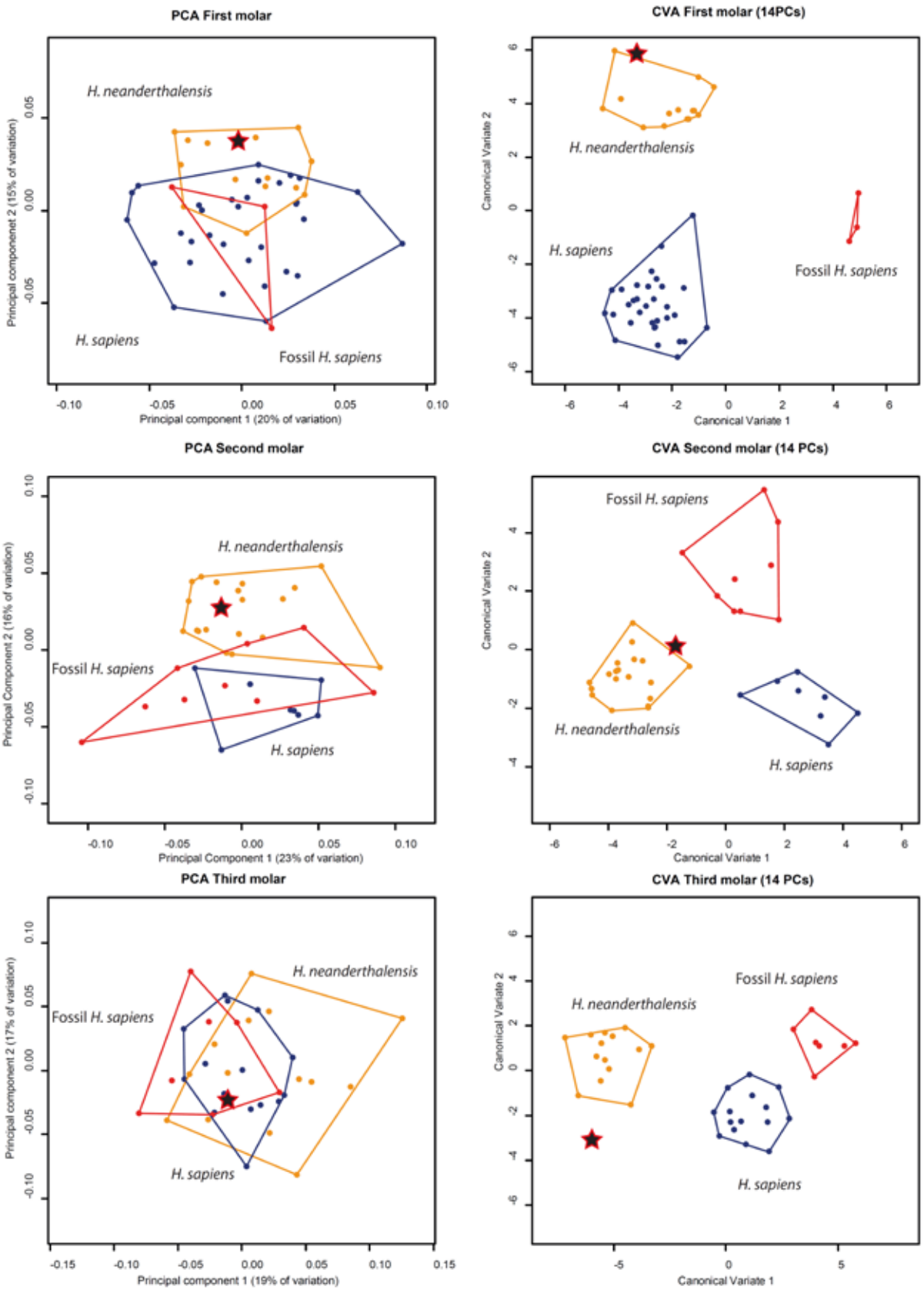

Figure 3: Principal component analysis and canonical variate analysis of EDJ shape in modern humans, Pleistocene Modern Humans and Neandertals for each mandibular molar.

age (i.e., Abri Suard 14-7 LRM_1; Krapina D1 LRM_2; Abri Suard 43 LRM_3, and Abri Suard 36 LLM_3: see Appendix 1). For the assessment of the classification of the Scladina specimens as Early or Classic Neandertals, these specimens were removed from the analysis.

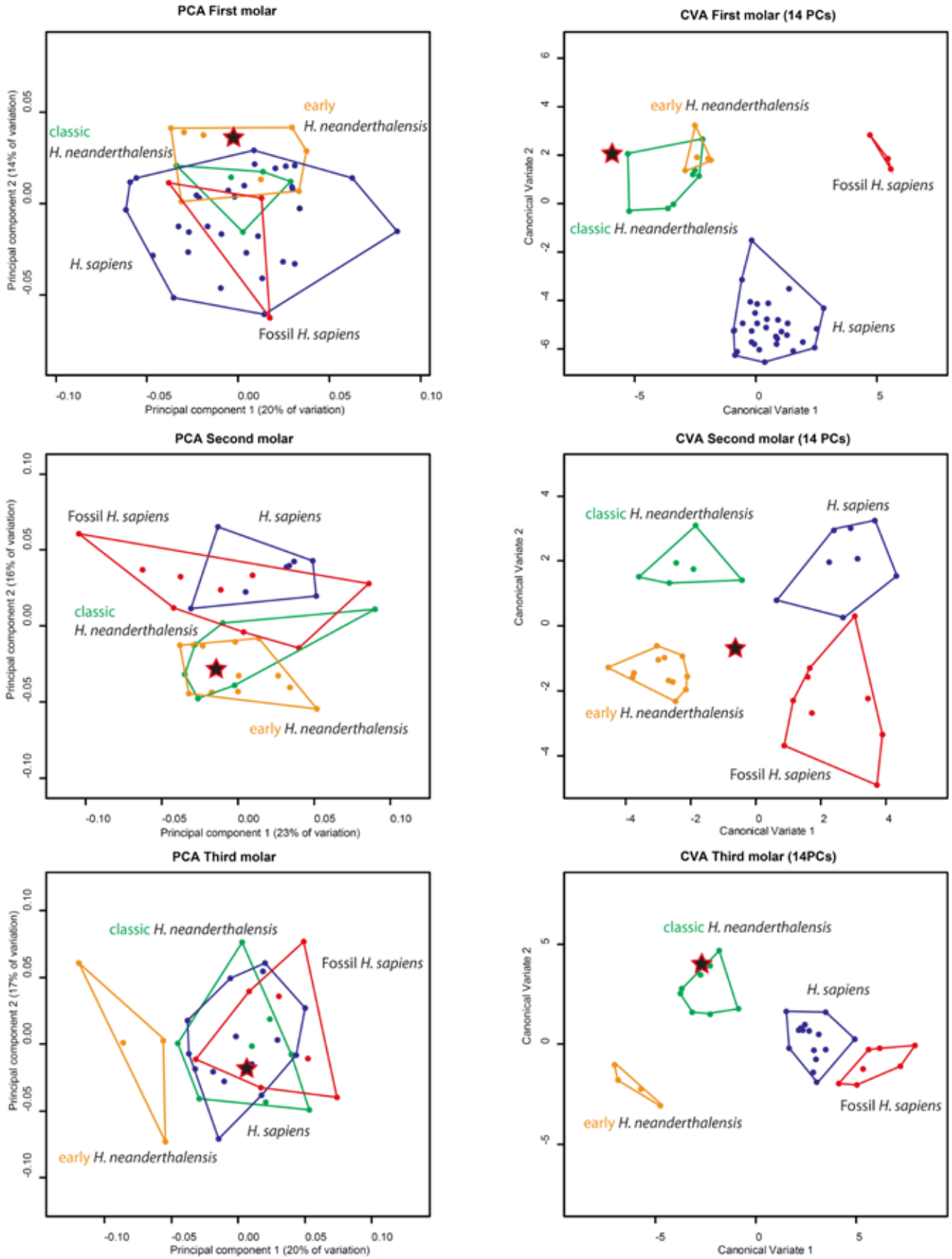

Figure 4: Principal component analysis and canonical variate analysis of EDJ shape for each mandibular molar and dividing the Neandertal sample into Early and Classic groups.

3.3. Comparison of Scladina I-4A with Early and Classic Neandertal morphotypes

In order to evaluate the affinity of Scladina with respect to Early and Classic Neandertal samples we excluded the ambiguously classified Neandertal specimens (see above). The M_1 of Scladina is classified as a Classic Neandertal (100%), the M_2 is classified as a Classic Neandertal 69% of the time, 19% as an Early Neandertal and the remaining times as a Pleistocene Modern Human (Figure 4). The M_3 is classified as a Classic Neandertal 63% of the time and as a Recent Modern Human 37% of the time (see Appendix 1).

The mean shape models of the different groups illustrate the subtle differences in Early and Classic Neandertal morphology (Figure 5). The Early morphology of the M_1 is characterised by a taller and more distally placed protoconid and a cervix that does not undulate in the occlusal-apical plane. The Classic morphology of the M_1 is characterised by a shorter and more mesially placed protoconid, and a cervix that dips in the middle of the lingual and buccal sides. Scladina shares with the classic morphotype the height of the protoconid and the dipping of the cervix along the lingual and buccal sides. For the M_2 and M_3 the differences in morphology between Early and Classic Neandertals are even more subtle. The Early morphotype of the M_2 is characterized by the more centrally placed entoconid, which Scladina shares. The Early morphotype of the M_3 is characterized by a slightly taller and more distally placed protoconid, a more distal location of both the hypoconid and entoconid, and a more mesially placed hypoconulid and distal ridge. The classic morphotype of the M_3 is characterized by a slightly shorter and more mesially placed protoconid, a more mesial location of both the hypoconid and the entoconid, and a more distally located hypoconulid and distal ridge. Scladina shares with the Early Neandertals the more mesially placed distal ridge, a protoconid height similar to that of the Classic Neandertals, but a protoconid position similar to Classic Neandertals.

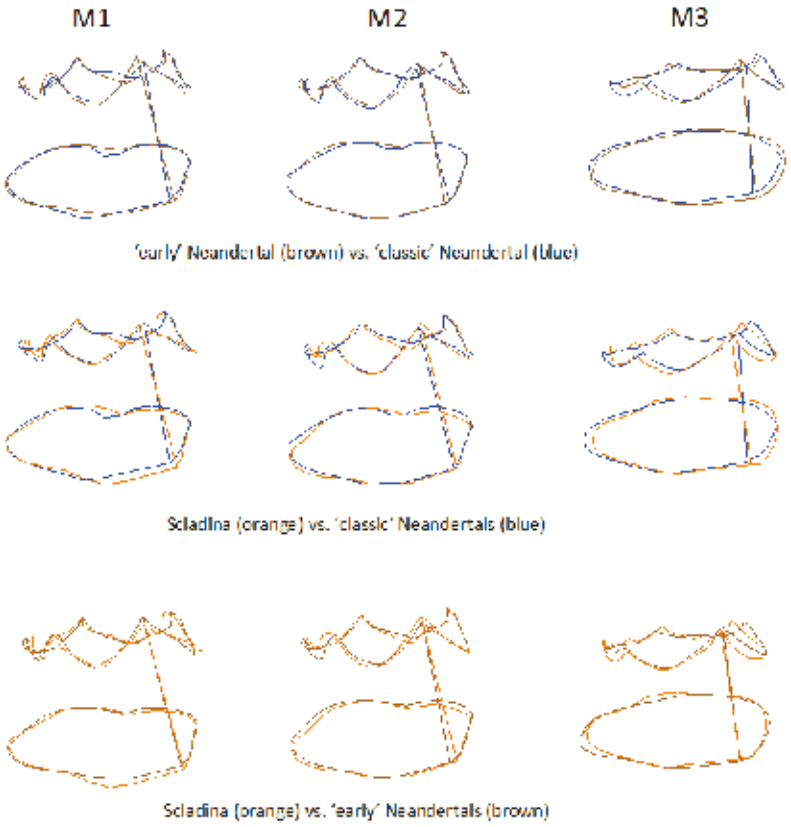

Figure 5: EDJ mean shape comparison between Scladina, Early Neandertals, and Classic Neandertals, shown from buccal side.

4. Discussion

Dating of Scladina has been problematic because of the complicated stratigraphy of the Sedimentary Complex 4 (Toussaint & Pirson, 2006), and has been estimated to 127 +46/-32ka by gamma spectrometry dating (Toussaint et al., 1998). However, it has recently been suggested that the best hypothesis would be to position the Scladina Neandertal remains in MIS 5b or MIS 5a (see Chapter 5). Each of the studied Scladina teeth is classified as a Classic Neandertal the majority of the time. As the date of Scladina is close to the cut-off point used in this study, 100ka, it is interesting to see that the EDJ morphology of Scladina aligns itself stronger with the Classic Neandertal sample than to the Early Neandertal sample.

The M_3 exhibits a greater variation in its morphology within species and greater overlap between species. This makes the M_3 less reliable when used in taxonomic classification studies as its results are less consistent compared to the classification results of M_1 or M_2. Therefore, the classification results of the Scladina M_3 as a modern human do not alter the taxonomic position of Scladina and can be attributed to the nature of the M_3 morphology in general.

The ambiguous classification of some Neandertal specimens compared to their geochronological age illustrates the continuous variation in morphology rather than the dichotomous distinction between two groups that has been tested here. This is illustrated by the oldest Neandertal specimens of our comparative sample, the Abri Suard individuals, not classifying consistently as Early Neandertals.

This demonstrates that as well as having a continuous variation instead of two separate groups, the temporal extremities of both the Early and Classic Neandertals exhibit significant variation as well. However, this study has shown that within the Neandertal continuum the differences in EDJ morphology are consistent enough to successfully distinguish between Early and Classic Neandertals.

5. Conclusion

This study confirms the Neandertal affinity of the Scladina specimen based on its EDJ morphology. The intraspecific taxonomic position of Scladina shows to be closer to that of the Classic Neandertal sample such as the El Sidron and Combe-Grenal specimens than to the Early Neandertal sample such as the Krapina and Abri Suard specimens. Furthermore, this study illustrates the presence of subtle yet consistent differences in EDJ morphology between the Early Neandertals and Classic Neandertals.

Acknowledgements

For access to specimens we thank the following institutions and individuals: Department of Archaeology, Belgrade University and the National Museum (Dušan Mihailović, Bojana Mihailović), Croatian National History Museum and the Croatian Academy of Science and Arts (Jakov Radovčić, Dejana Brajković); Francisc J. Rainer Institute of Anthropology (Andrei Dorian Soficaru); Geologisch-Paläontologisches Institut der Universität Heidelberg (Ullrich A. Glasmacher); Institut National des Sciences de l'Archéologie et du Patrimoine (A. Ben-Ncer, M. A. El Hajraoui, F. Z. Sbihi-Alaoui); Musée Archéologique de Rabat (S. Raoui); Iziko South African Museum (access to specimen from Fred Grine, scanning by Paul Tafforeau); Musée d'Archéologie Nationale de Saint-Germain-en-Laye (Patrick Périn); Musée d'Angoulême (Jean-François Tournepiche); Musée d'Art et d'Archéologie du Périgord (Véronique Merlin-Langlade); Musée National de Préhistoire, Les Eyzies-de-Tayac (Jean-Jacques Cleyet-Merle); Museo Nacional de Ciencias Naturales (Antonio Rosas); Museum für Vor- und Frühgeschichte Berlin (Almut Hoffmann); National Museum of Natural History (David Hunt); Rockefeller Museum Jerusalem (Alegre Savariego and Ibrahim Fawzi); Royal Belgian Institute of Natural Sciences; Sackler School of Medicine (Israel Hershkovitz, Yoel Rak, Alon Barash); Senckenberg Forschungsinstitut und Naturmuseum (Ottmar Kullmer and Friedemann Schrenk); TNT/NESPOS (Roberto Macchiarelli); Michel Toussaint; Universität Leipzig; Institut für Anatomie, Lehrsammlung Anatomie (Christine Feja) and Jean-Jacques Hublin's private collection; University Mohammed V-Agdal (Mohamed Boutakiout). For technical assistance we thank Adeline Le Cabec, Collin Moore, Robin Feeney, Tanya Smith, Kornelius Kupczik, and Simon Neubauer. For scanning assistance we thank Heiko Temming and Patrick Schoenfeld.

References

Bailey S. E., 2002. A closer look at Neanderthal postcanine dental morphology: the mandibular dentition. *The Anatomical Record, The New Anatomist*, 269: 263–299.

Bailey S. E., 2006. Beyond shovel-shaped incisors: Neandertal dental morphology in a comparative context. *Periodicum Biologorum*, 108: 253–267.

Corrucini R. S., 1987. The Dentinoenamel junction in primates. *International Journal of Primatology*, 8: 99–114.

Corruccini R. S. 1998. The dentino-enamel junction in primate mandibular molars. In J. R. Lukacs (ed.), *Human dental development, morphology, and pathology: a tribute to Albert A. Dahlberg*. Portland, University of Oregon, Anthropological Papers: 1–16.

Dean D., Hublin J.-J., Holloway R. & Ziegler R., 1998. On the phylogenetic position of the pre-Neanderthal specimen from Reilingen, Germany. *Journal of Human Evolution*, 34: 485–508.

Garralda M.-D., Vandermeersch B., 2000. The Neanderthals from Combe-Grenal cave (Domme, Dordogne, France). *Paleo*, 12: 213–259.

Gower J. C., 1975. Generalized Procrustes analysis. *Psychometrika*, 40: 33–51.

Grine F. E., 2004. Description and preliminary analysis of new hominid craniodental remains from the Swartkrans Formation. In C. K. Brain (ed.), *Swartkrans: A Cave's Chronicle of Early Man*. Pretoria, Transvaal Museum: 75–116.

Guatelli-Steinberg D. & Irish J. D., 2005. Early hominin variability in first molar dental trait frequencies. *American Journal of Physical Anthropology*, 128: 477–484.

Gunz P., Mitteroecker P. & Bookstein F. L., 2005. Semilandmarks in three dimensions. In D. E. Slice (ed.), *Modern Morphometrics in Physical Anthropology*. New York, Kluwer Academic/Plenum Publishers: 73–98.

Gunz P., Ramsier M., Kuhrig M., Hublin J.-J. & Spoor F., 2012. The mammalian bony labyrinth reconsidered,

introducing a comprehensive geometric morphometric approach. *Journal of Anatomy*, 220: 529–543.

Harvati K., Hublin J.-J. & Gunz P., 2010. Evolution of middle-late Pleistocene human cranio-facial form: A 3-D approach. *Journal of Human Evolution*, 59, 5: 445–464.

Harvati K., Panagopoulou E. & Karkanas P., 2003. First Neanderthal remains from Greece: the evidence from Lakonis. *Journal of Human Evolution*, 45: 465–473.

Hlusko L. J., 2004. Protostylid variation in *Australopithecus*. *Journal of Human Evolution,* 46: 579–594.

Hublin J.-J., 1998. Climatic changes, paleogeography and the evolution of Neanderthals. In K. Aoki & O. Bar-Yosef (eds.), *Neanderthals and Modern Humans in Western Asia.* Plenum Press, New York: 295–310.

Hublin J.-J. 2009. The origin of Neandertals. *Proceedings of the National Academy of Sciences of the United States of America*, 106, 38: 16022–16027.

Irish J. & Guatelli-Steinberg D., 2003. Ancient teeth and modern human origins: an expanded comparison of African Plio-Pleistocene and recent world dental samples. *Journal of Human Evolution,* 45: 113–144.

Johanson D. C., 1974. *An odontological study of the chimpanzee with some implications for hominoid evolution*. Unpublished PhD thesis, University of Chicago.

Macchiarelli R., Bondioli L., Debénath A., Mazurier A., Tournepiche J.-F., Birch W & Dean C., 2006. How Neanderthal molar teeth grew. *Nature*, 444: 748–751.

Olejniczak A. J., Giblert C. C., Martin L. B., Smith T. M., Ulhaas L. & Grine F. E., 2007. Morphology of the enamel-dentine junction in sections of anthropoid primate maxillary molars. *Journal of Human Evolution,* 53: 292–301.

Olejniczak A. J., Martin L. B. & Ulhaas L., 2004. Quantification of dentine shape in anthropoid primates. *Annals of Anatomy*, 186: 479–485.

Pilbrow V., 2003. *Dental variation in African apes with implications for understanding patterns of variation in species in fossil apes*. Unpublished PhD thesis, New York University.

Pilbrow V., 2006. Population systematics of chimpanzees using molar morphometrics. *Journal of Human Evolution*, 51: 646–662.

Radovčić J., Pomtykalo D. & Wolpoff M. H., 1988. *The Krapina Hominids: an illustrated catalog of skeletal collection.* Zagreb, Mladost Publishing House.

Robinson J. T., 1956. *The Dentition of the Australopithecinae*. Pretoria, Transvaal Museum. Memoir No 9, 179 p.

Rohlf F. J. & Slice D., 1990. Extensions of the Procrustes method for the optimal superimposition of landmarks. *Systematic Zoology,* 39: 40–59.

Skinner M. M., 2008. *Enamel-dentine junction morphology in extant hominoid and fossil hominin lower molars*. Unpublished PhD thesis, George Washington University.

Skinner M. M., Gunz P., Wood B. A., Boesch C. & Hublin J.-J., 2010. Discrimination of extant *Pan* species and subspecies using the enamel-dentine junction morphology of lower molars. *American Journal of Physical Anthropology*, 140: 234–243.

Skinner M. M., Gunz P., Wood B. A. & Hublin J.-J., 2008. Enamel-dentine junction (EDJ) morphology distinguishes the lower molars of *Australopithecus africanus* and *Paranthropus robustus. Journal of Human Evolution*, 55: 979–988.

Skinner M. M., Wood B. A. & Hublin J.-J., 2009. Protostylid expression at the enamel-dentine junction and enamel surface of mandibular molars of *Paranthropus robustus* and *Australopithecus africanus*. *Journal of Human Evolution*, 56: 76–85.

Sperber G., 1974. *Morphology of the cheek teeth of early South African hominids*. Unpublished PhD thesis, University of Witwatersrand.

Suwa G., 1996. Serial allocations of isolated mandibular molars of unknown taxonomic affinities from the Shungura and Usno formations, Ethiopia, a combined method approach. *Human Evolution*, 11: 269–282.

Suwa G., Kono R. T., Katoh S., Asfaw B. & Beyene Y., 2007. A new species of great ape from the late Miocene epoch in Ethiopia. *Nature*, 448: 921–924.

Teilhol V., 2001. *Contribution à l'étude individuelle des ossements d'enfants de la Chaise de Vouthon (Charente, France): approche paléodémographique, paléoethnologique, aspect morphologique et étude métrique. Place phylognique des enfants de la Chaise.* Unpublished PhD thesis, University of Perpignan.

Toussaint M., Otte M., Bonjean D., Bocherens H., Falguères C. & Yokoyama Y., 1998. Les restes humains neandertaliens immatures de la couche 4A de la grotte Scladina (Andenne, Belgique). *Comptes rendus de l'Académie des Sciences de Paris, Sciences de la terre et des planètes*, 326: 737–742.

Toussaint M. & Pirson S., 2006. Neandertal Studies in Belgium: 2000-2005. *Periodicum Biologorum*, 108, 3: 373–387.

Uchida A., 1992. *Intra-species variation among the great apes: implications for taxonomy of fossil hominoids*. Unpublished PhD thesis, Cambridge, Harvard University.

Uchida, A., 1996. *Craniodental Variation among the Great Apes*. Peabody Museum. Bulletin 4, Cambridge, Harvard University Press.

Weidenreich F., 1937. The dentition of *Sinanthropus pekinensis*: a comparative odontography of the hominids. *Palaeontologia Sinica*, Series D, 1: 1–180.

Wood B. A. & Abbott S. A., 1983. Analysis of dental morphology of Plio-Pleistocene hominids. I. Mandibular molars: crown area measurements and morphological traits. *Journal of Anatomy*, 136: 197–210.

Specimen	Tooth	Date	Expected	Early Hn	Classic Hn	Hs	Fossil Hs
Lakonis_LLM3	LM3	<38–44ka	Classic	0	16	0	0
Le Moustier LLM1	LM1	40ka	Classic	0	16	0	0
Le Moustier LLM2	LM2	40ka	Classic	0	16	0	0
Le Moustier LLM3	LM3	40ka	Classic	0	16	0	0
Saint-Césaire LRM3	LM3	40ka	Classic	0	16	0	0
Vindija 11_39 LRM2	LM2	45–35ka	Classic	0	16	0	0
Vindija 11_39 LRM3	LM3	45–35ka	Classic	4	12	0	0
El Sidron SD1135 LRM3	LM3	49–39ka	Classic	0	15	1	0
El Sidron SD540 LLM2	LM2	49–39ka	Classic	0	16	0	0
El Sidron SD755 LRM2	LM2	49–39ka	Classic	0	16	0	0
El Sidron SD780_LLM1	LM1	49–39ka	Classic	2	14	0	0
Combe-Grenal I LRM1	LM1	70ka	Classic	0	16	0	0
Combe-Grenal XII LLM3	LM3	70ka	Classic	0	16	0	0
Combe-Grenal IV LLM1	LM1	70ka	Classic	0	16	0	0
Le Regourdou LLM2	LM2	70ka	Classic	0	16	0	0
Le Regourdou LLM3	LM3	70ka	Classic	0	16	0	0
La Quina H9 LLM2	LM2	71–60ka	Classic	0	16	0	0
La Quina H9 LLM3	LM3	71–60ka	Classic	0	16	0	0
Roc de Marsal LRM1	LM1	90–60ka	Classic	0	16	0	0
Scladina 4A–1 LRM1	**LM1**	**100ka**	**?**	**0**	**16**	**0**	**0**
Scladina 4A–1 LRM2	**LM2**	**100ka**	**?**	**3**	**11**	**0**	**2**
Scladina 4A–1 LRM3	**LM3**	**100ka**	**?**	**0**	**10**	**6**	**0**
Krapina 52 LLM1	LM1	130ka	Early	16	0	0	0
Krapina 53 LRM1	LM1	130ka	Early	16	0	0	0
Krapina 53 LRM2	LM2	130ka	Early	16	0	0	0
Krapina 53 LRM3	LM3	130ka	Early	16	0	0	0
Krapina 54 LLM1	LM1	130ka	Early	16	0	0	0
Krapina 54 LLM2	LM2	130ka	Early	16	0	0	0
Krapina 55 LLM1	LM1	130ka	Early	15	0	0	1
Krapina 55 LLM2	LM2	130ka	Early	16	0	0	0
Krapina 57 LRM3	LM3	130ka	Early	16	0	0	0
Krapina 79 LRM1	LM1	130ka	Early	16	0	0	0
Krapina 81 LLM1	LM1	130ka	Early	15	1	0	0
Krapina D1 LRM2	LM2	130ka	Early	10	6	0	0
Krapina D104 LRM3	LM3	130ka	Early	16	0	0	0
Krapina D105 LLM2	LM2	130ka	Early	16	0	0	0
Krapina D106 LLM3	LM3	130ka	Early	16	0	0	0
Krapina D107 LLM2	LM2	130ka	Early	16	0	0	0
Krapina D6 LLM2	LM2	130ka	Early	16	0	0	0
Krapina D80 LRM2	LM2	130ka	Early	14	2	0	0
Krapina D86 LLM2	LM2	130ka	Early	16	0	0	0
Krapina D9 LLM2	LM2	130ka	Early	16	0	0	0
Krapina 57 LRM2	LM2	130ka	Early	16	0	0	0
Krapina 59 LRM2	LM2	130ka	Early	16	0	0	0
Abri Suard 14 7 LRM1	LM1	185–101ka	Early	9	7	0	0
Abri Suard 36 LLM3	LM3	185–101ka	Early	11	5	0	0
Abri Suard 36 LLM2	LM2	185–101ka	Early	16	0	0	0
Abri Suard 43 LRM3	LM3	185–101ka	Early	6	10	0	0
Abri Suard 49 LRM1	LM1	185–101ka	Early	15	1	0	0
Abri Suard 5 LLM1	LM1	185–101ka	Early	14	2	0	0

Appendix 1: Classification results for the complete Neandertal sample using PC 5-20. Specimens that have been highlighted in grey have been removed from the sample as they were classified ambiguously. Early Hn = Early *Homo neanderthalensis*, Classic Hn = Classic *Homo neanderthalensis*, Hs = *Homo sapiens*, Fossil Hs = Fossil *Homo sapiens*.